Spin-cluster effect and lattice-deformation-induced Kondo effect, spin-glass freezing, and strong phonon scattering in $La_{0.7}Ca_{0.3}Mn_{1-x}Cr_xO_3$

Bai-Mei Wu,[a] Bo Li, and Wei-Hua Zhen
Structural Research Laboratory, Department of Physics, University of Science and Technology of China, Hefei 230036, People's Republic of China

M. Ausloos
Services Universitaires Pour la Recherche et les Applications Technologiques des Materiaux Electrocéramiques, Composites et Supraconducteurs (SUPRATECS), Institut de Physique B5, Universite de Liege, B-4000 Liege, Belgium

Ying-Lei Du
Department of Astronomy and Applied Physics, University of Science and Technology of China, Hefei 230036, People's Republic of China

J. F. Fagnard and Ph. Vanderbemden
Services Universitaires Pour la Recherche et les Applications Technologiques des Materiaux Electrocéramiques, Composites et Supraconducteurs (SUPRATECS), Institut de Electricite, Montefiore B28, Universite de Liege, B-4000 Liege, Belgium

(Received 27 September 2004; accepted 8 March 2005; published online 4 May 2005)

Besides the Kondo effect observed in dilute magnetic alloys, the Cr-doped perovskite manganate compounds $La_{0.7}Ca_{0.3}Mn_{1-x}Cr_xO_3$ also exhibit Kondo effect and spin-glass freezing in a certain composition range. An extensive investigation for the $La_{0.7}Ca_{0.3}Mn_{1-x}Cr_xO_3$ ($x=0.01$, 0.05, 0.10, 0.3, 0.6, and 1.0) system on the magnetization and ac susceptibility, the resistivity and magnetoresistance, as well as the thermal conductivity is done at low temperature. The spin-glass behavior has been confirmed for these compounds with $x=0.05$, 0.1, and 0.3. For temperatures above T_f (the spin-glass freezing temperature) a Curie–Weiss law is obeyed. The paramagnetic Curie temperature θ is dependent on Cr doping. Below T_f there exists a Kondo minimum in the resistivity. Colossal magnetoresistance has been observed in this system with Cr concentration up to $x=0.6$. We suppose that the substitution of Mn with Cr dilutes Mn ions and changes the long-range ferromagnetic order of $La_{0.7}Ca_{0.3}MnO_3$. These behaviors demonstrate that short-range ferromagnetic correlation and fluctuation exist among Mn spins far above T_f. Furthermore, these interactions are a precursor of the cooperative freezing at T_f. The "double bumps" feature in the resistivity-temperature curve is observed in compounds with $x=0.05$ and 0.1. The phonon scattering is enhanced at low temperatures, where the second peak of double bumps comes out. The results indicate that the spin-cluster effect and lattice deformation induce Kondo effect, spin-glass freezing, and strong phonon scattering in mixed perovskite $La_{0.7}Ca_{0.3}Mn_{1-x}Cr_xO_3$. © *2005 American Institute of Physics*. [DOI: 10.1063/1.1898438]

I. INTRODUCTION

The perovskite manganese oxide has again become an interesting object since this material shows some exotic electronic transport and magnetic properties as well as colossal magnetoresistance (CMR),[1–5] which is known to be one of the future resources in detecting and recording magnetic signals. In $R_{1-x}A_xMnO_3$ (R=rare earth, A=Ca, Sr, Ba, and Pb) system, for the particular content of the manganates, the mixed valency (Mn^{3+}/Mn^{4+}) leads to a strong ferromagnetic (FM) interaction that arises from a double-exchange (DE) mechanism.[6] A metal-insulator (MI) transition and CMR occur at and around the ferromagnetic Curie temperature (T_C). Besides DE interaction the lattice distortion is believed to play an important role through strong electron-lattice coupling, which arises from the Jahn–Teller (JT) distortion around Mn^{3+} ions.[7–12] It is generally recognized that the study of Mn-site doping is expected to provide important clues to the mechanism of CMR. During the recent years, there have been more and more reports on the effects of Mn-site doping with foreign elements.[13–20] It is found that Mn-site doping generally decreases the Curie temperature and the MI transition temperature. However, the exact effect depends on the nature of the doped elements. Among these doped elements, Cr has a rather slow decreasing effect on the Curie temperature and the MI transition temperature.[21–24] Moreover, some extraordinary phenomena, for example, the spin-glass-like freezing in magnetism[25,26] and "double bumps" in resistivity[21,27,28] are observed in doped compounds. All the phenomena are interesting and attractive, but it is hard to extract the exact explanation because of the complex interplay among charge, lattice, and spin in the prototype CMR material $La_{0.7}Ca_{0.3}MnO_3$. In this paper, we report our measurements on dc magnetization, ac susceptibility, magnetotransport, and thermal conductivity for the

[a]Electronic mail: wubm@ustc.edu.cn

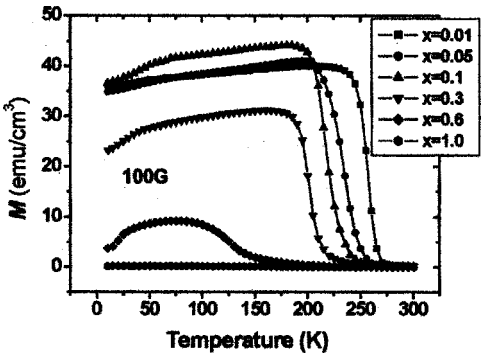

FIG. 1. ZFC magnetization vs temperature $M(T)$ in a field of 100 G for $La_{0.7}Ca_{0.3}Mn_{1-x}Cr_xO_3$.

perovskite $La_{0.7}Ca_{0.3}Mn_{1-x}Cr_xO_3$ ($x=0.01$, 0.05, 0.10, 0.3, 0.6, and 1.0). Kondo effect and spin-glass freezing have been well confirmed in this system in certain composition ranges. An enhanced phonon scattering is almost simultaneous with the second bump of double bumps in resistivity. The results indicate that the spin-cluster effect and lattice deformation induce Kondo effect, spin-glass freezing, and strong phonon scattering in mixed perovskite $La_{0.7}Ca_{0.3}Mn_{1-x}Cr_xO_3$.

II. EXPERIMENTS

A series of polycrystalline samples $La_{0.7}Ca_{0.3}Mn_{1-x}Cr_xO_3$ ($x=0.01$, 0.05, 0.10, 0.3, 0.6, and 1.0) were prepared by the conventional solid-state reaction method.[29] Appropriate amounts of $La_2O_3, CaCO_3, MnO_2$, and Cr_2O_3 were mixed and heated in air at 900 °C for 24 h, and then heated at 1200 °C for 24 h with intermediate grinding. After the powder was pressed into pellets, a final sintering was carried out at 1400 °C for 24 h. The structure and phase purity of samples were checked by powder x-ray diffraction (XRD) with Cu K_α radiation at room temperature. The XRD patterns prove that all samples are single phase in orthorhombic perovskite structure.

All measurements on electrical transport and magnetism were performed by a Physical Property Measurement System (PPMS) of Quantum Design from 5 to 300 K. In the zero-field cool (ZFC) measurements the sample was cooled down from room temperature to 5 K before a measured field was applied. In the field cool (FC) measurements the sample was cooled in an applied field from room temperature to 5 K. All the magnetization data, $M_{\mathrm{ZFC}}(T)$ and $M_{\mathrm{FC}}(T)$, were collected in warming the sample up to 300 K. AC susceptibility measurements were carried out in an applied field $H_{\mathrm{ac}}=10$ G at different frequencies from 10 to 1003 Hz. The resistivity in magnetic field up to 7.0 T was measured by the standard four-probe method. The thermal conductivity data were measured by the method of longitudinal steady thermal flow.[30]

III. RESULTS

A. Magnetization and ac susceptibility

The M_{ZFC}, as a function of temperature T in the field of 100 G for all the $La_{0.7}Ca_{0.3}Mn_{1-x}Cr_xO_3$ ($x=0.01$, 0.05, 0.10, 0.3, 0.6, and 1.0) samples, is presented in Fig. 1. The form of the curves is qualitatively similar to that described for the manganites by many authors. The paramagnetic-ferromagnetic phase transition occurs around T_C, the Curie temperature confirmed by the magnetization measurement. T_C is suppressed slowly with the increase of Cr (for $x \leqslant 0.3$) that is shown in Table I. The sample with $x=0.6$ shows a lower hillside in the magnetization, probably associated with an antiferromagnetic transition. For the end member, $x=1.0$, M has a tiny temperature-independent diamagnetic contribution. The magnitude of M increases at lower doping ($x \leqslant 0.1$) and then goes down when the Cr content is $x>0.1$.

TABLE I. Experimental values on magnetic and transport properties of $La_{0.7}Ca_{0.3}Mn_{1-x}Cr_xO_3$.

x	T_C (K)	θ (K)	T_{MI} (K)	T_f (K)	T_k (K)
0.01	264	265	264		265
0.05	250	250	245	78	260
0.1	233	250	225	70	240
0.3	213	250		45	
0.6		205			

The $M_{\mathrm{ZFC}}(T)$ and $M_{\mathrm{FC}}(T)$ curves in the field of 25 G are presented in Fig. 2 for $La_{0.7}Ca_{0.3}Mn_{1-x}Cr_xO_3$ ($x=0.01$, 0.10, and 0.3). Irreversibility between the ZFC and FC magnetization curves is clearly seen close to T_C for all Cr-doped samples. The thermomagnetic irreversibility arises from the magnetic anisotropy[18] or is due to spin-glass-like behavior as reported in many-order magnetic systems. However, the results indicate no simple ferromagnetic long-range order in these Cr-doped compounds. The drop of the $M_{\mathrm{ZFC}}(T)$ at lower temperatures deserves attention and may be related to the interaction between spins (see the following).

The ac susceptibility measurements are a compatible technique usually used to search for the magnetic glass behavior in a material. The susceptibility will have two components: a real part $\chi'(\omega)$, the dispersion, and an imaginary part $\chi''(\omega)$, the absorption. The temperature dependence of $\chi'(T)$ and $\chi''(T)$ is measured at the frequency of 73 Hz and is displayed in Fig. 3 for $La_{0.7}Ca_{0.3}Mn_{1-x}Cr_xO_3$ ($x=0.01$, 0.05, 0.10, 0.3, 0.6, and 1.0). The temperature dependence of $\chi'(T)$ shows a maximum at high temperatures and a bend at low temperatures. The maximum should be the paramagnetic-ferromagnetic transition observed in dc $M_{\mathrm{ZFC}}(T)$ curves, and the bend may be qualitatively explained

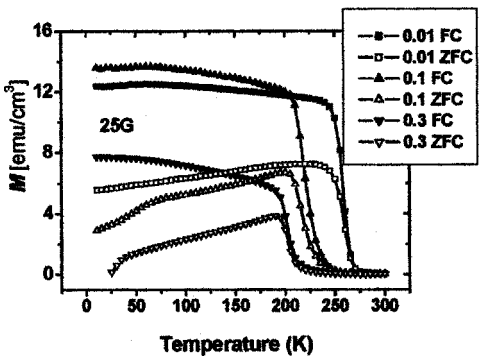

FIG. 2. Magnetization vs temperature $M(T)$ in ZFC (circle) and FC (solid circle) processes in a field of 25 G for $La_{0.7}Ca_{0.3}Mn_{1-x}Cr_xO_3$.

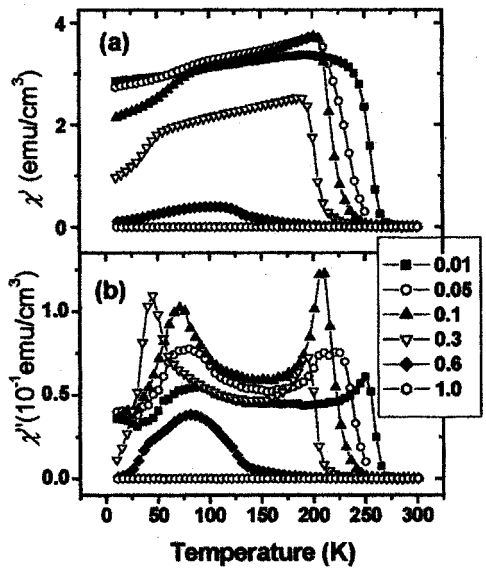

FIG. 3. Temperature dependence of ac susceptibility (a) χ' and (b) χ'' in applied field $H_{ac}=10$ Oe at 73 Hz for $La_{0.7}Ca_{0.3}Mn_{1-x}Cr_xO_3$.

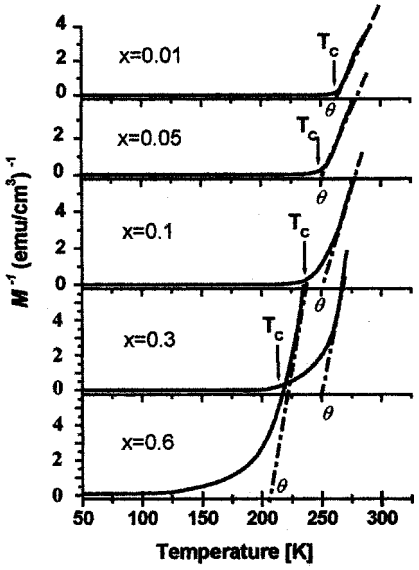

FIG. 5. Reciprocal susceptibility of $La_{0.7}Ca_{0.3}Mn_{1-x}Cr_xO_3$ as a function of temperature.

in the same way as the drop in dc $M_{ZFC}(T)$. There exist two peaks in the $\chi''(T)$ curve. One peak at high temperature appears at the same temperature related to the paramagnetic-ferromagnetic transition and its position in the temperature coordinate is independent of frequency. The other sharp cusp is located at low temperatures. More important is that the position of this cusp in the temperature coordinate is dependent on frequency and shifts to higher temperature when the frequency of the ac field increases from 10 to 1003 Hz. Typical results are displayed in Fig. 4 for the sample with $x=0.1$. The frequency shift offers a good criterion for distinguishing a canonical spin glass from a superparamagnet. At the same time the cusp is depressed (not shown) when a dc field is applied from 0 to 500 G. All these phenomena are the typical features of spin glass.[31] The spin-freezing temperature T_f can, thus, be determined and is listed in Table I. Table I shows the important parameters obtained from the magnetic and transport measurements.

The sharp cusp appearing in ac susceptibility is a common character of spin glass. This is a visible representation of spin freezing in a macroscopic scale. In fact each interaction responsible for spin freezing has affected the physical properties at far higher temperatures than T_f.[31,32] We plot the data measured in the paramagnetic phase as M^{-1} versus T in Fig. 5 for the different Cr content x. The susceptibility of $La_{0.7}Ca_{0.3}Mn_{1-x}Cr_xO_3$ compounds exhibits deviation from Curie–Weiss behavior $[M/H=C/(T-\theta)]$ at relatively high temperatures, where the curves clearly show different values of the Curie constants and the paramagnetic Curie temperature θ that is also listed in Table I. θ represents a sum of all the exchange interaction for a completely random system. The value of θ is reduced as x increases and maintains nearly a constant value for $x=0.05$, 0.1, and 0.3, and is then reduced with increasing Cr, which reflects a decay of local ferromagnetism. Thus, the ferromagnetic exchanges are becoming more improbable as Cr substitution increases.

B. Resistivity and magnetoresistivity

Figure 6 shows the temperature dependence of resistivity, $\rho(T)$, for $La_{0.7}Ca_{0.3}Mn_{1-x}Cr_xO_3$ ($x=0.01$, 0.05, 0.10, 0.3, 0.6, and 1.0) samples measured in zero field. All members have an insulating behavior at room temperature. Cr-doped manganates with $x\leqslant 0.1$ have a transition to the metallic state at T_{MI} that is listed in Table I. When the doping is in excess of 0.3, the insulating state is maintained. The double

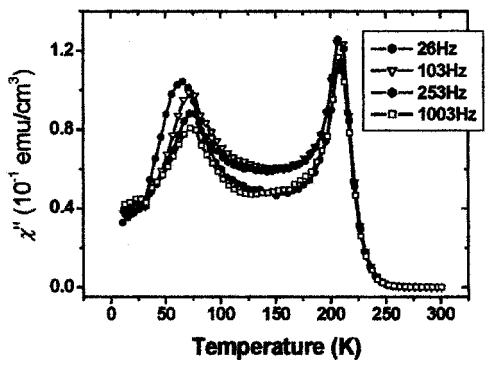

FIG. 4. AC susceptibility measured at different frequencies

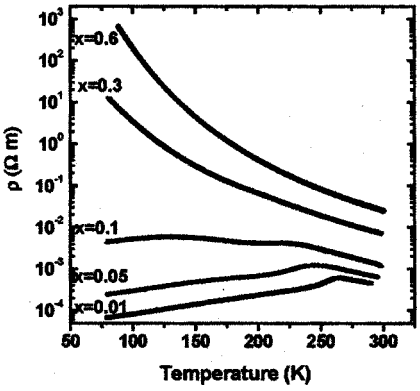

FIG. 6. Temperature dependence of resistivity for $La_{0.7}Ca_{0.3}Mn_{1-x}Cr_xO_3$.

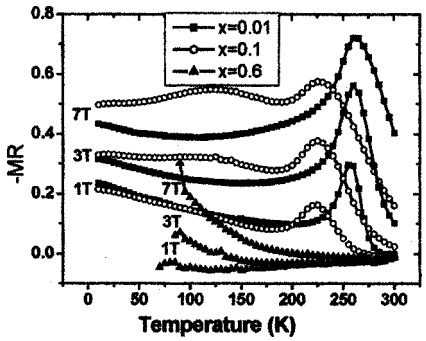

FIG. 7. MR as a function of temperature under 1, 3, and 7 T.

bumps feature in $\rho(T)$ curve is observed in samples with $x=0.05$ and 0.1, which is consistent with what has been reported.[21] We suppose that it is a consequence of a possible competition between the single-impurity Kondo effect and the Ruderman–Kittel–Kasuya–Yosida (RKKY) interaction, and we will discuss it in details thereinafter.

The magnetoresistivity *MR* measured in the fields of 1, 3, and 7 T as a function of temperature is shown in Fig. 7. *MR* is defined as

$$MR = [R(H) - R(0)]/R(0), \tag{1}$$

where $R(H)$ is the value of the resistivity in an applied field H. *MR* is negative for the Cr-doped samples, but it displays a little positive in lower fields of 1 T for a sample with $x=0.6$. For the end member, $La_{0.7}Ca_{0.3}CrO_3$, no *MR* is detected even if the fields are applied up to 8 T. It should be noticed that the nature of *MR* for Cr-doped manganates is somewhat different from the pure manganate, $La_{0.7}Ca_{0.3}MnO_3$. For the Cr-doped manganates *MR* extends broadly over the temperature range investigated. In addition, a small field can induce a modest *MR* at lower temperatures, as is seen in Fig. 7.

To show clearly the double bumps in $R(T)$ we magnify these features in Fig. 8 for the sample with $x=0.1$. One of the double bumps at the high temperature, which is related to MI transition, arises from acknowledged DE, the other puts up a very large peak around 130 K. Below the double bumps is a minimum resistivity. Furthermore, upon applying a field the resistance of the compound is suppressed drastically in the whole temperature range, meanwhile the position of the minimum in $R_H(T)$ curves is maintained. This resistance

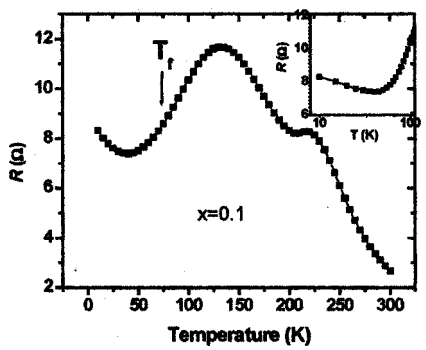

FIG. 8. Temperature dependence of resistivity for the sample with $x=0.1$. The inset shows R plotted as a function of logarithmic T.

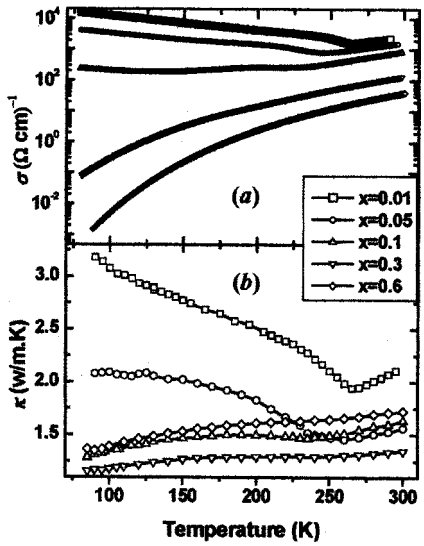

FIG. 9. Temperature dependence of (a) electrical conductivity and (b) thermal conductivity for $La_{0.7}Ca_{0.3}Mn_{1-x}Cr_xO_3$.

minimum behavior in $La_{0.7}Ca_{0.3}Mn_{0.9}Cr_{0.1}O_3$ may be attributed to the Kondo effect that is generally observed in dilute magnetic alloys.[33] Kondo describes this phenomena based on the *s-d* interaction model between a single magnetic impurity (d) and the conduction electrons (s), which gives rise to a singular term in the resistivity involving $c \log T$ as a factor, where c is the concentration of impurity atoms. Combined with the lattice resistivity, the outcome is a resistance minimum, provided the *s-d* exchange integral J is negative. In Fig. 8 we show, in the inset, R plotted as a function of logarithmic T. The Kondo effect in Cr-doped manganates then is possible. Applied magnetic fields suppress the spin-flip scattering of the conduction electrons, thus leading to a negative magnetic resistance.

C. Thermal conductivity

The temperature dependence of thermal conductivity $\kappa(T)$ is shown in Fig. 9(b) for the $La_{0.7}Ca_{0.3}Mn_{1-x}Cr_xO_3$ ($x=0.01$, 0.05, 0.10, 0.3, and 0.6) samples. On the whole, behaviors of the $\kappa(T)$ curves are consistent, as reported in some perovskite manganese oxides.[34–38] The value of κ is gradually reduced with increasing Cr, except when $x=0.6$. The $\kappa(T)$ at high temperatures above T_C decreases as temperature is reduced, and the respective slope $d\kappa/dT$ almost remains constant, which is definitely positive for all samples. A sharp increase of thermal conductivity at temperature, named T_k, corresponding to MI transition is found for samples with $x \leqslant 0.1$. The values of T_k shift to low temperatures with the Cr doping and are listed in Table I. Moreover, for samples with $x=0.05$ and 0.1, $\kappa(T)$ is suppressed dramatically over a low temperature range below T_C, where the second bump in $\rho(T)$ comes out.

The thermal conductivity $\kappa(T)$ in general is contributed by electrons (κ_e) and phonons (κ_{ph}),

$$\kappa(T) = \kappa_e(T) + \kappa_{ph}(T). \tag{2}$$

According to the Wiedemann–Franz law, we can estimate the electron contribution κ_e from the resistivity data,

$$\kappa_e(T) = L_0 T\sigma, \tag{3}$$

where the Lorenz constant $L_0 = 2.45 \times 10^{-8}$ W Ω/K^2 and σ is the electrical conductivity. The contributions of κ_e in all samples are estimated to be less than 1% of the total thermal conductivity and can be negligible. Thus $\kappa(T)$ is almost entirely due to phonons in the present samples.

IV. DISCUSSION

The compounds, $La_{0.7}Ca_{0.3}Mn_{1-x}Cr_xO_3$ for finite x, can be considered as a $La^{3+}{}_{0.7}Ca^{2+}{}_{0.3}Cr^{3+}{}_xMn^{3+}{}_{0.7-x}Mn^{4+}{}_{0.3}O_3$ composite. The substitution of Cr for Mn sites induces antiferromagnetic interaction between Cr^{3+}–O–Cr^{3+} and promotes the proportion of Mn^{4+}–O–Mn^{4+}; combined with ferromagnetic double-exchange interaction of Mn^{3+}–O–Mn^{4+}, there always exist mixed magnetic interactions in $La_{0.7}Ca_{0.3}Mn_{1-x}Cr_xO_3$. Doping with Cr does not change the electron concentration in the samples, but it dilutes the magnetic interaction between Mn ions as the x in $Mn_{0.7-x}Cr_x$ increases. This leads to the decrease in the probability of ferromagnetic coupling between Mn ions of nearest neighbors. The neutron powder diffraction study of the richly doped manganite with Cr on Mn site reveals that Mn and Cr form antiferromagnetic zigzag chains along the a axis.[39] The randomness of the spins of the neighboring coupling, ferromagnetic or antiferromagnetic, predominates in the system when a given Mn ion has Cr ions as a significant fraction of its nearest neighbors. Ultimately, when Cr ions neighbor each other for the higher doping of Cr, one might expect their mutual interaction to dominate. The anomaly in the magnetic and transport properties for x around 0.1 thus signifies a crossover.

We suppose that spin clusters with antiferromagnetic order grow and are imbedded in the ferromagnetic matrix below T_C, which induces a complicated spin-cluster effect. Irreversibility and time-dependent effects observed in magnetic measurements have proven this point. With decreasing temperature the ferromagnetic and antiferromagnetic competing interactions finally make the magnetic coupling constant in the system, which goes into a spin-glass state. The available theories focus upon the freezing of already existing clusters at T_f. Nevertheless, the spin correlations far above T_f are very important and must be considered.[31,32] The development of these correlations generates the spin-glass state. This interpretation is consistent with the varying θ in our results if we naively assume that this interaction strength is proportional to the number of Mn ions without a Cr neighbor. We notice in Fig. 5 that the value of θ is reduced as x is increased, then maintains a nearly constant value for samples with $x = 0.05$, 0.1, and 0.3. In those Cr-doped samples the spin-glass behavior has been confirmed. That is to say, the main effect of Cr doping is to decrease θ by decreasing Mn ions in the sample, thereby introducing less ferromagnetic exchange in the system. Short-range correlations and fluctuations exist among spins of Mn ions, and these interactions are a precursor to the lower-temperature spin-glass freezing.

The electrical transport exhibits no transition at the spin-freezing temperature, only a gradual transformation (see Fig. 8). The frozen state is random, and the frozen disorder will still make a significant contribution to the scattering. Certainly, the spin-disorder scattering is steadily reduced when the temperature is lowered through T_f. What we seem to be detecting at temperatures above T_f, namely, the broad bump in the $\rho(T)$ curves below T_C (for example, around 130 K for $x = 0.1$ in Fig. 8) may be the long tail of the Kondo effect, which has a negative temperature coefficient. The change in sign of the slope in the $\rho(T)$ curves represents a competition between the single-impurity Kondo effect which causes a resonant scattering and the RKKY interaction that wants to couple the spin, thereby reducing the spin-disorder scattering. All these occur above T_f and as a precursor to it.[31] Again, contrasted with the temperature dependence of electrical resistivity and susceptibility, the second bump below T_C in $\rho(T)$ and the valley in $\chi''(T)$ are present at the same temperature. The results can be explained such that conduction electrons come under a *spin-dependent* scattering.[40] Applied magnetic fields restrain the energy of spin coupling and promote the conductivity that leads to CMR. The magnetic-sensitive resistivity occurs in a wide temperature range. Thus, the resistive transition is no longer related purely to the magnetism, but rather to the scatters caused by the spin-cluster effect that generally consists of spin-glass matrices. The influence of spin-cluster effect on transport properties is expected to be rather important. Some work has been done on studying various possible scenarios,[41,42] including the splitting of phase transitions due to the occurrence of magnetic clusters.

Concerning phonon thermal conductivity, we pay attention to the similar temperature dependencies of $\kappa(T)$ and electrical conductivity $\sigma(T)$ around MI transition in Figs. 9(a) and 9(b). The comparability of $\kappa(T)$ and $\sigma(T)$ is indirectly related to the electron (charge)-lattice coupling and is tuned by the state of the charge carriers. The electron processes will induce a displacement of large Jahn–Teller distorted (d^4) MnO_6 octahedron by undistorted (d^3) octahedron. Although the anharmonic distortions exist in both metallic and insulating regimes,[34] the local lattice distortion is different due to the different states of charge carriers. In the metallic state, the electrons are itinerant, the dynamic electron processes will urge the distortion of (d^4) MnO_6 octahedron to be uniformly averaged over neighboring undistorted (d^3) MnO_6 octahedron. Lattice polarons will not tend to form. On the contrary, electrons are localized in the insulating state, electron processes are weaker and e_g electrons are easier to trap in (d^4) MnO_6 octahedra, so that the lattice polarons are easier to form. In the viewpoint of phonon transportation, the lattice polarons are the scattering centers of phonons. Hence, the phonon thermal conduction has a relationship with the state of charge carriers. Another origin for the phonon scattering may be expected at low temperatures due to spin-dependent scattering. Since the anomalous enhancement in phonon scatter is almost simultaneous with the second bump in $\rho(T)$ in a wide temperature range below T_C for samples with $x = 0.05$ and 0.1,[40] it is possible that some mechanisms closely related to spin-cluster effect–lattice interaction are the origin of the enhancement. Both the local fluctuation of the lattice structure related with the state of charge carriers

and the spin-cluster effect related with the state of spin coupling act upon the phonon transport. These results indicate the importance of electron(charge)-phonon interaction and spin-phonon interaction in Cr-doped $La_{0.7}Ca_{0.3}Mn_{1-x}Cr_xO_3$ system.

V. CONCLUSION

We have presented the temperature dependence of the dc magnetization, ac susceptibility, resistivity, magnetoresistivity, and thermal conductivity in a Cr-doped $La_{0.7}Ca_{0.3}Mn_{1-x}Cr_xO_3$ ($x=0.01$, 0.05, 0.10, 0.3, 0.6, and 1.0) series. The spin-glass behavior has been confirmed for this compound with $x=0.05$, 0.1, and 0.3. For temperatures far above T_f a Curie–Weiss law is obeyed. The paramagnetic Curie temperature θ is dependent on Cr doping. Doping with Cr dilutes Mn-ion nearest neighbors and weakens ferromagnetic exchange in the system. The short-range correlations and fluctuations existing among the Mn spins at high temperature are a precursor to the lower-temperature spin-glass freezing at T_f. Below T_f there exists a Kondo minimum in resistivity. The colossal magnetoresistance occurs in this system with the doping concentration of Cr up to $x=0.6$. The double bumps feature in the $\rho(T)$ curve is observed in samples with $x=0.05$ and 0.1 and is regarded as a consequence of a possible competition between the single-impurity Kondo effect and the RKKY interaction. The phonon scattering is enhanced at low temperatures, where the second peak of double bumps in $\rho(T)$ comes out. Analyses on phonon thermal transport indicate the strong scatter caused by the local fluctuation of the lattice structure and the spin-cluster effect, which reveals the possible importance of the electron(charge)-phonon and spin-phonon interactions in mixed perovskite $La_{0.7}Ca_{0.3}Mn_{1-x}Cr_xO_3$.

ACKNOWLEDGMENTS

This work is supported by the National Nature Science Foundation of China (Grant No. 10174070) and the Belgium National Fund for Scientific Research (FNRS) under Grant No. FRFC 2.4590.01.

[1] S. Jin, T. H. Tiefel, M. Meconnack, R. A. Fastnacht, R. Ramesh, L. H. Chen, Science **264**, 413 (1994).
[2] R. V. Helmolt, J. Wecker, B. Holzapfel, L. Schultz, and K. Samwer, Phys. Rev. Lett. **71**, 2331 (1993).
[3] K. Chahara, T. Ohno, M. Kasai, and Y. Kosono, Appl. Phys. Lett. **63**, 1990 (1993).
[4] A. P. Ramirez, J. Phys.: Condens. Matter **9**, 8171 (1997).
[5] For more detailed discussions and extensive references, see *Colossal Magnetoresistance, Charge Ordering, and Related Properties of Manganese Oxides*, edited by C. N. R. Rao and B. Raveau (World Scientific, Singapore, 1988); J. M. D. Coey, M. Viret, and S. Von Molnar, Adv. Phys. **48**, 167 (1999); *Localized to Itinerant Electronic Transitions in Perovskite Oxides*, edited by J. B. Goodenough (Springer, Berlin, 2001); E. Dagotto, *Nanoscale Phase Separation and Colossal Magnetoresistance: The Physics of Manganites and Related Compounds*, Springer Series in Solid State Sciences Vol. 136 (Springer, Berlin, 2003).
[6] C. Zener, Phys. Rev. **82**, 403 (1951).
[7] J. S. Zhou and J. B. Goodenough, Phys. Rev. Lett. **80**, 2665 (1998).
[8] A. J. Millis, Nature (London) **392**, 147 (1998).
[9] H. Y. Hwang, S.-W. Cheong, P. G. Radaelli, M. Marezio, and B. Batlogg, Phys. Rev. Lett. **75**, 914 (1995).
[10] H. Roder, J. Zang, and A. R. Bishop, Phys. Rev. Lett. **76**, 1356 (1996).
[11] W. H. Zheng, B. M. Wu, D. S. Yang, J. Y. Li, X. R. Liu, and B. Li, Chin. J. Low Temp. Phys. **23**, 216 (2001).
[12] P. Wagner, I. Gordon, S. Mangin, V. V. Moshchalkov, Y. Bruynseraede, L. Pinsard, and A. Revcolevschi, Phys. Rev. B **61**, 529 (2000).
[13] F. Rivadulla, M. A. López-Quintela, L. E. Hueso, P. Sande, J. Rivas, and R. D. Sanchez, Phys. Rev. B **62**, 5678 (2000).
[14] K. Ghosh, S. B. Ogale, R. Ramesh, R. L. Greene, T. Venkatesan, K. M. Gapchup, R. Bathe, and S. I. Patil, Phys. Rev. B **59**, 533 (1999).
[15] I. O. Troyanchuk, M. V. Bushynski, N. V. Pushkarev, H. Szymczak, and K. Barner, J. Magn. Magn. Mater. **235**, 331 (2001).
[16] H. Song, W. Kim, S.-J. Kwon, and J. Kang, J. Appl. Phys. **89**, 3398 (2001).
[17] N. Gayathri, A. K. Raychaudhuri, S. K. Tiwary, R. Gundakaram, A. Arulraj, and C. N. R. Rao, Phys. Rev. B **56**, 1345 (1997).
[18] D. C. Kundaliya, R. Vij, R. G. Kulkarni, A. A. Tulapurkar, R. Pinto, S. K. Malik, and W. B. Yelon, J. Magn. Magn. Mater. **264**, 62 (2003).
[19] Y. Moritomo, A. Machida, S. Mori, N. Yamanoto, and A. Nakamura, Phys. Rev. B **60**, 9220 (1999).
[20] K. Suzuki, H. Fujishiro, Y. Kashiwada, Y. Fujine, and M. Ikebe, Physica B **329–333**, 922 (2003).
[21] Y. Sun, X. Xu, and Y. Zhang, Phys. Rev. B **63**, 054404 (2001).
[22] R. Ganguly, I. K. Gopalakrishnan, and J. V. Yakhmi, Physica B **275**, 308 (2000).
[23] O. Cabeza, O. Barca, G. Francesconi, M. A. Bari, C. Severack, C. M. Muirhead, and F. Miguelez, J. Magn. Magn. Mater. **196–197**, 504 (1999).
[24] O. Cabeza, M. Long, C. Severac, M. A. Bari, C. M. Muirhead, M. G. Francesconi, and C. Greaves, J. Phys.: Condens. Matter **11**, 2569 (1999).
[25] Z. H. Wang *et al.*, J. Appl. Phys. **85**, 5399 (1999).
[26] J. W. Cai, C. Wang, B. G. Shen, J. G. Zhao, and W. S. Zhan, Appl. Phys. Lett. **71**, 1727 (1997).
[27] G. H. Rao, J. R. Sun, Y. L. Zhang, and J. K. Liang, J. Phys.: Condens. Matter **8**, 5393 (1996).
[28] G. Li, X. Ze, C. O. Kim, H. J. Kim, and Y. W. Lee, J. Magn. Magn. Mater. **239**, 51 (2002).
[29] W. H. Zheng, B. M. Wu, B. Li, D. S. Yang, and L. Z. Cao, Chin. J. Low Temp. Phys. **24**, 230 (2002).
[30] B. M. Wu, D. S. Yang, B. Li, W. H. Zheng, and S. Sheng, Chin. J. Low Temp. Phys. **25**, 248 (2003).
[31] J. A. Mydosh, *Spin Glass: An Experimental Introduction* (Taylor & Francis, London, 1993).
[32] A. F. J. Morgownik and J. A. Mydosh, Phys. Rev. B **24**, 5277 (1981).
[33] J. Kondo, Prog. Theor. Phys. **32**, 37 (1964).
[34] D. W. Visser and A. P. Ramirez, Phys. Rev. Lett. **78**, 3947 (1997).
[35] M. Ikebe and H. Fujishiro, J. Phys. Soc. Jpn. **67**, 1083 (1998).
[36] H. Fujishiro and M. Ikebe, Physica B **263–264**, 691 (1999).
[37] C. Hess and B. Büchner, Phys. Rev. B **59**, R10397 (1999).
[38] Y. Kashiwada, H. Fujishiro, and M. Ikebe, Physica B **329–333**, 924 (2003).
[39] E. Gamari-Seale, *E-MRS Fall Meeting 2003, Symposium D, Invited Oral*.
[40] B.-M. Wu, M. Ausloos, Y.-L. Du, W.-H. Zheng, B. Li, J. F. Fagnard, and Ph. Vanderbemden, Chin. Phys. Lett. **22**, 686 (2005).
[41] S. Sergeenkov, H. Bougrine, M. Ausloos, and A. Gilabert, Phys. Rev. B **60**, 12322 (1999).
[42] M. Ausloos, L. Hubert, S. Dorbolo, A. Gilabert, and R. Cloots, Phys. Rev. B **66**, 174436 (2002).